11106 *J. Phys. Chem. A* **2000,** *104,* 11106−11110

Ab Initio Computational Study of Environmentally Harmful Gasoline Additives: Methyl *tert*-Butyl Ether and Analogues

Laura N. Gregerson, Jay S. Siegel, and Kim K. Baldridge*

San Diego Supercomputer Center, La Jolla, California 92093-0505, and Department of Chemistry, University of California—San Diego, La Jolla, California 92093-0358

Received: June 7, 2000; In Final Form: July 31, 2000

MTBE (methyl *tert*-butyl ether), a widely used gasoline additive, is recently being scrutinized for potential environmental damage in groundwater and in the atmosphere. This study is a first-level investigation of the basic structure and properties of MTBE and various analogues, as well as an analogous class of amines, as a first step toward understanding the reactions of such species in the environment. The gas-phase structures and properties have been calculated using a variety of ab initio methods, including correlated Hartree−Fock and hybrid density functional theory methodologies. Results are discussed in light of known experimental and environmental phenomena. Accurate fundamental results are projected to aid experimental studies and provide insight into potential mechanisms of action, the latter of which will be the second level of investigation by this group. Eventual proposals of more effective gasoline additives are targeted.

Introduction

Methyl *tert*-butyl ether (MTBE) is used as an oxygenate additive in reformulated gasoline and oxyfuels.[1,2] Other examples of such oxygenate additives include ethanol (EtOH) and ethyl *tert*-butyl ether (ETBE). These oxygenates aid in the reduction of carbon monoxide and hydrocarbon emissions as required by the Clean Air Act.[3] Although the Clean Air Act does not specify which oxygenate should be used, MTBE is chosen more often because it is cost-effective, mixes well with gasoline, and can be transported through existing pipelines.[4] The EPA has recently classified MTBE as a possible cancer-causing agent.[5] Toxicity[6] and carcinogenicity[7,8] studies have linked MTBE to actual human illness. Because of its potential toxicity, a few states, including California and Maine, have begun to consider phasing out MTBE from their gasoline altogether. As such, there is recent interest in the potential health and environmental risks associated with oxygenates such as MTBE,[6] as well as the need for more effective, less harmful oxygenates.

Although the problem of groundwater and surface water contamination by motor vehicle fuels and fuel additives is not new, the issues associated with fuels containing oxygenates show particular characteristics. Oxygenates are added to fuels to increase the oxygen content, thereby reducing undesirable emissions from the fuel. The issues with MTBE predicate from the fact that, unlike hydrocarbons, which get tied up in humin adsorption and clay, it is soluble in water. Thus, MTBE moves in soils, rivers, lakes, and underground water supplies. Water quality studies performed by the U.S. Geological Survey (USGS) indicate concentrations of MTBE in the range from 0.2 μg/L to over 20 000 μg/L [1 μg/L = 1 part per billion (ppb)].[9] Key drinking sources in California have reported contamination of drinking water at well over 100 μg/L.[10] In addition, MTBE only slowly bioremediates and is resistant to oxidative processes. For example, MTBE does not react with ozone, and reacts with OH radical at a rate of 2.94×10^{-12} cm^3/(molecule s),[11] implying long lifetime in the environment. MTBE is known to be volatile and readily undergoes UV-initiated decomposition in the atmosphere.[12]

To assess the potential for oxygenates such as MTBE to pose significant threat to human health or the environment, it is necessary to fully characterize such contaminants. However, until recently, very limited and relatively inconsistent data existed for such contaminants, either experimentally or theoretically. Early experimental studies focused on spectroscopic properties.[13−15] More recent work has involved investigations into agents that may remove MTBE from water sources,[16] and understanding the reaction processes in the atmosphere.[11,17,18] These latter studies include the oxidation of MTBE by ozone and peroxone processes, both of which leave other possible contaminants in the water.

Understanding photochemical reactions of oxygenate additives and their impact on the environment is crucial in the monitoring of air quality and ozone depletion. Because of its fundamental importance, the OH radical initiated oxidation of MTBE and its impact on the reactivity of automobile emissions in the troposphere are the focus of theoretical and experimental studies.[13−15] Complicated mechanisms have been suggested (Figure 1) and investigated experimentally,[11,17,18] but there are no current theoretical studies of these processes, and because of this complexity, many aspects of this reaction have yet to be revealed.

In this work, we present accurate determination of the structure and properties of MTBE as well as several analogues of MTBE, including ethyl *tert*-butyl ether (ETBE) (another oxygenate additive), di-*tert*-butyl ether (DTBE), and their heavy isotopomers. These results are compared with an analogous class of amines. Results are discussed in light of known experimentally[7,8] and theoretically determined[14] quantities, and give insights into our further dynamics and solution-phase studies.

Computational Methods

All calculations have been carried out using the GAMESS,[19,20] and Gaussian98[21] software packages. The computations employ a variety of levels of theory for comparative purposes. Wavefunction-based methods considered include Hartree−Fock meth-

10.1021/jp002055t CCC: $19.00

TABLE 1: Calculated Structural Parameters for MTBE[a]

basis set	<(COC)	*r*(C_1−O)	*r*(C_9–C_6)	*r*(C_7−C_6)	<(C_9CO)	<(C_9CC_7)	*r*(C_6−O)
HF/4-21G[e]	119.1	1.440	1.533	1.538	102.6	110.5	1.459
HF/6-31G*	119.7	1.394	1.527	1.532	103.6	110.0	1.416
HF/DZ+(2d,p)	119.6	1.393	1.527	1.532	104.0	109.8	1.416
MP2/DZ+(2d,p)	116.2	1.419	1.526	1.532	103.3	110.1	1.440
MPW1PW91/DZ+(2d,p)	117.5	1.403	1.526	1.530	103.7	110.0	1.431
B3PW91/DZ+(2d,p)	117.6	1.406	1.528	1.533	103.6	110.0	1.435
B3LYP/DZ+(2d,p)	118.0	1.412	1.533	1.539	103.5	110.1	1.442
ED[i]	118.9	1.415[d]	1.532[b]		103.1[c]	111.1[b]	1.448
MOCED[e]	119.1	1.422	1.530	1.534	103.4[f]	110.6	1.441
ED[g]	115.8	1.412	1.533[b]		102.9	111.1[b]	1.429
MS[h]	118.5	1.415[d]	1.498	1.567	106.3	110.4	1.417[d]

[a] Distances are in angstroms; angles are in degrees. [b] Only average values are reported. [c] Calculated from δ and <(CCC). [d] Fixed value. [e] Reference 28. [f] Calculated from values of <(C_7CO), <(C_9CC_7), and <(C_8CC_7). [g] Reference 31. [h] Reference 42. [i] Reference 43.

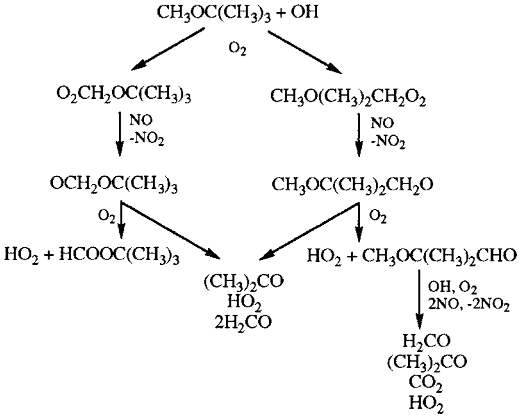

Figure 1. Photochemical reaction processes involving oxygenate additives.

ods,[22] second-order Møller−Plesset perturbation theory (MP2) methods,[23,24] and hybrid density functional theory (HDFT) methods,[25] which constitute a known improvement over “pure” DFT methods via inclusion of the exact Hartree−Fock exchange based on Kohn−Sham orbitals.[26,27] Gradient corrections for exchange were applied via the three-parameter hybrid functional of Becke,[28] whereas for correlation the functionals derived by Lee et al.[29] or Perdew,[30] respectively, were employed (usually abbreviated as B3LYP and B3PW91). Additionally, the more recent Barone and Adamos Becke-style one-parameter functional using modified Perdew−Wang exchange and Perdew−Wang 91 correlation, MPW1PW91, was explored.[31] For discussion of the effect of basis sets on structure and energetic properties, a variety of basis sets have been employed. These include 6-31G-(*nd,mp) [n* = *1, 2; m* = 0, 1],[32−35] DZV(2d,p), and DZ+(2d,p),[36] as well as Dunning’s correlation consistent basis sets up to cc-pVTZ.[37,38] These correlated levels have been shown to be good post-Hartree−Fock treatment of systems with varying levels of van der Waals types of interactions. At each optimized geometry, the Hessian (matrix of second derivative) was calculated to determine local minima (positive definite) or an nth-order saddle point (n negative eigenvalues). Visualization and analysis employed QMView[39] and MacMolPlt.[40] Vibrational frequencies and assignment of orbital energies, based on the Δ(SCF) approximation,[41] have been performed at the B3LYP/DZ+(2d,p) level of theory.

Discussion

The general classes of ethers and amines studied in this work are illustrated in Figure 2. The minimum-energy structure of MTBE is shown in Figure 3. The minimum-energy structure found for MTBE possesses C_s symmetry, in agreement with experiment[13,15] and previous low-level ab initio calculations.[14] Several geometric parameters describing this structure are reported in Table 1. The known experimentally determined parameters in this table are in disagreement with each other, due to the variety of techniques and level of approximation made therein.

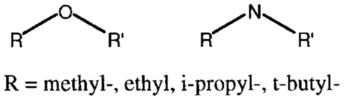

Figure 2. Schematic of general classes of ethers and amines.

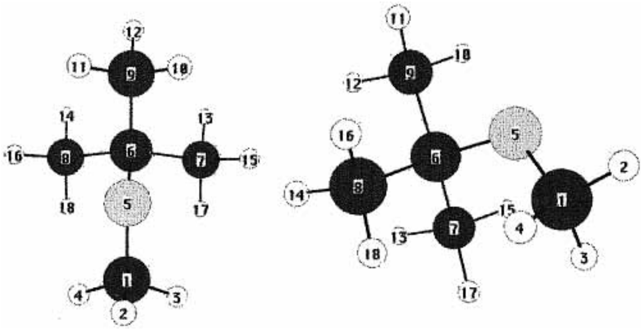

Figure 3. Calculated structure of MTBE.

Of particular interest is the detailed description of the structure and properties of MTBE, as an aid in understanding the mechanistic aspects of its role in groundwater contamination as well as atmospheric reactions. The ability to predict these properties reliably is of great importance, especially due to the difficulties associated with the experimental procedures. To address the issue of reliability and provide a quantum mechanical reference with which to compare experimentation data, computations on MTBE have been performed at a variety of levels of theory (Table 1). This exhaustive basis set and method analysis on MTBE has the added benefit of establishing an accurate methodology with which to pursue the full analysis of both the ether and amine classes of compounds. The understanding of the results of structural variations in these sets of compounds can aid in the pursuit of environmentally clean oxygenates, and perhaps in finding ways to clean up existing MTBE problems in either the air or water.

The parameters that are most affected by a change in basis set and correlation methodology are the CO bond length and the COC angle. Convergence at the RHF level predicts a COC bond angle of 119.6° and a CO bond length of 1.416 Å (RHF/DZ+(2d,p); Table 1). The result of increasing basis set size beyond what has been reported in the literature (RHF/4-21G-(d)) is a significant improvement in these two parameters as well as several others, with most of the improvement coming

TABLE 2: Comparison of Ether and Amine Structural Features

param	DME	MTBE	DTBE	MTBA	DMA	DTBA
r(CX)	1.412 (1.415)[d]	1.442	1.442 (1.436)[e]	1.480	1.460 (1.456)[f]	1.481 (1.469)[g]
r(CC)[b]		1.537	1.540 (1.532)[e]	1.541		1.545 (1.561)[g]
∠(CXC)	112.6 (111.8)[d]	118.0	127.6 (130.8)[e]	117.9	112.9 (112.0)[f]	127.6 (135.0)[g]
∠(CCC)[b]		110.3	109.4 (110.5)[e]	109.4		108.3
tilt[c]		5.0	7.0 (7.0)[e]	3.4		5.7 (2.5)[g]

[a] Distances are in angstroms; angles are in degrees. All ab initio structures of ethers calculated at B3LYP/DZ+(2d,p); experimental values, where available are shown in parentheses. See Table 1 for MTBE experimental values. [b] Average. [c] Tilt angle defined as $(2/3)(<(C_{asym}CX) - <(C_{sym}CX))$.[43] [d] Reference 43. [e] Reference 28. [f] Reference 38. [g] Reference 14.

from a better representation of the valence shells, rather than due to extensive polarization functionality. There is, in fact, very little change in structural parameters with the addition of various types of polarization functions. After consideration of basis set convergence as established at the RHF level of theory, the effects of dynamic correlation have been investigated with the same DZ+(2d,p) basis set (Table 1). This was done at the MP2 and HDFT methodologies, the latter applying several of the more current functionals. Dynamic correlation of any type tends to decrease the COC bond angle by up to 3°, and increase the CO bond length by close to 0.03 Å. It is interesting to note the variation in predictability between the three HDFT functionals. While the newer 1-parameter functional, MPW1PW91, and the B3PW91 functional predict almost identical structural values, the B3LYP functional predicts a slightly longer C−O stretch and a slightly larger COC angle bend.

The available experimentally determined structures for MTBE is subject to notable discrepancy. Of the values reported, those predicted by Konaka's molecular orbital constrained electron diffraction (MOCED) studies and the electron diffraction studies of Suwa[13,42] make the fewest assumptions in their procedure and are closest to the "best" computation reported here (B3LYP/DZ+(2d,p)). The remaining two experimental studies shown in Table 1 fixed the CO bond parameters to deduce the final structure,[14,15] because these values being poorly determined by the experimental procedure.

Several studies of X(t-Bu$)_2$ (X = N, O, C) show that "sterically demanding" tert-butyl groups influence several structural parameters of a molecule with respect to their unhindered analogues.[43] In fact, one can investigate this phenomenon within a series of substituted ethers (Figure 2). Table 2 shows structural data from a variety of ether analogues with (a) R, R′ = methyl, methyl, (b) R, R′ = methyl, *tert*-butyl, and (c) R, R′ = *tert*-butyl, *tert*-butyl, respectively. Within this grouping, one ascertains an "all-or-nothing" effect on CX with *tert*-butyl substitution, going from 1.412 Å in dimethyl ether to 1.442 Å with either one or two substituted *tert*-butyl groups. Although the CX bond length is the same in the latter two, the associated COC angle is drastically changed to accommodate the sterics involved, changing from 118.0 in MTBE to 127.6 in DTBE.

An interesting comparison can be made of the series of ethers with a similar series of amine structures. Table 2 shows the structural parameters for an analogous set of amine analogues. One would expect the steric strain to be slightly less in amines than in ethers due to the single lone pair on nitrogen in the former case, versus the two sets of lone pairs on oxygen in the latter. While the CN bond length in DMA is approximately 0.05 Å longer than in DME, the increase in this bond length upon replacement of one of the methyl groups by a *tert*-butyl group is only 0.02 Å, compared to the 0.03 Å seen in the ether series. No appreciable bond lengthening accompanies the transition to DTBA. With the progressive increase in *tert*-butyl substitution, the CNC angle changes by the same magnitude as did the COC angle in the ether series. Given the smaller force constant for C−N vs C−O wagging modes (0.3640 vs 0.3843 mdyn/Å, for MTBA and MTBE, respectively, calculated at B3LYP/DZ+(2d,p)), one can conclude that a slightly smaller strain is present in the amines.

TABLE 3: B3LYP/DZ+(2d,p) Calculated CXC Angle of Select Ethers and Amines

ROR' RNHR'	Me	Et	i-Pr	t-Bu
Me	112.6 112.9	113.0	116.9	118.0
Et	113.3	113.3 113.8	117.4	118.5
i-Pr	116.9	117.4	116.1 118.0	119.5
t-Bu	117.9	118.5	119.7	127.6 127.6

This relatively small increase in the CX bond lengths relative to the much larger variations in the $C_RXC_{R'}$ bond angle in both cases follows directly from the larger force constant for stretching vs bending distortions (e.g., 1.036 vs 0.3843 mdyn/Å for stretching and bending in MTBE, respectively). In the equilibrium structures, there is a balance between steric and electronic distortions. The nonbonded steric repulsion between the alkyl groups is relieved by the lengthening of the CX bond and widening of the CXC angle. Electronic forces come into play with the increase in s character in the X−C bonds and p character in the lone pairs, as the angle opens.

In addition to the distortions of the bond and the angles, internal strain can also be distributed within distortions of the *tert*-butyl groupings. These groups tend to adopt conformations in comparison to the dimethyl analogue, such that the opposing C_t-Bu−C bonds are essentially staggered and tilted away from each other. The substantial tilt angle is a clear indicator of the inability of a CXC angle distortion to balance the nonbonded repulsion between the alkyl groups. The extensive distortions throughout the *tert*-butyl derivatives also help to explain the problems associated with experimental determinations of the structure of MTBE.[44] Table 3 shows a more complete set of CXC angles for all possible R, R′ substitutions within the ether and amine series. It is clear from this table, with one exception (R=R′ = i-Pr), that the respective structures have near identical angle deformations in all cases.

Ionization Potentials. Ionization potentials (IPs) are approximated using the Δ(SCF) method[41] at the B3LYP/

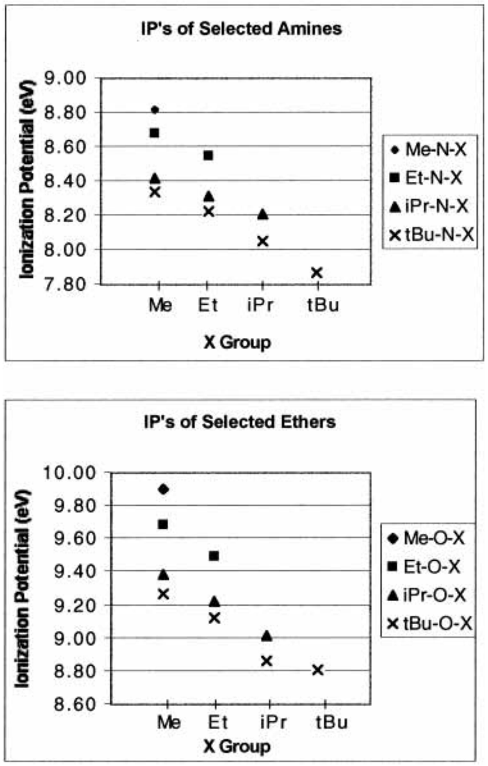

Figure 4. (a, top) Ionization potentials of select amines (Δ(SCF) calculated at B3LYP/DZ+(2d,p), eV). (b, bottom) Ionization potentials of select ethers (Δ(SCF) calculated at B3LYP/DZ+(2d,p), eV).

DZ+(2d,p) level of theory. Trends in ionization potential are projected to have implications on the mechanism of reactivity of MTBE. Calculated results (Figure 4) show similar trends of decreasing IP as the ether or amine is more highly substituted. As the IP decreases, the corresponding CXC angle tends to increase. This angle opening induces the lone pairs on X to rehybridize, giving them more p-character, and consequently making the molecule easier to oxidize. The 0.7 eV decrease in IP for DME vs MTBE promotes the possibility of a mechanism of 1-electron transfer out of O to radical cation, versus direct ether attack in the environmental or decomposition chemistry of MTBE. Equally indicative is the increase in basicity of amines with facile IPs.

Dipole Moment. Calculating the rotational constants and electric dipole moment accurately is of great importance for our further studies involving the effects of solvation on MTBE and various analogues. Accurate prediction of dipole and higher multipole moments is essential for reliable predictions of the structure and properties in solvated conditions. Because of the sp^2-like hydrogen on the nitrogen, the amine lone pair has more p-character as the molecule approaches a planar geometry. As the electronegativities of H and C are comparable, the N−C and N−H bond vectors almost cancel in the plane. The ethers retain a bent geometry with a clear δ^+/δ^- orientation. Therefore, we can expect amines to have lower dipole moments than their ether analogues (Table 4), and potentially overall lower solvation energies. Within the ether series, MTBE has the third largest dipole (methyl isopropyl ether being the largest), which would imply a larger degree of solvation, one of the harmful features of MTBE leakage into water sources.

Conclusions

Because of its potential toxicity, a few states, including California and Maine, have begun consideration of the phasing out of MTBE from their gasoline all together. As more states look for alternatives to this source of gasoline oxidant, remediation against existing MTBE in the environment will be of general concern. This increased interest in the potential health and environmental risks associated with MTBE, as well as the established difficulties associated with experimental studies of such processes, will benefit from computationally derived chemical and physical properties such as presented in this work. These as well as further studies will enhance the understanding of the reactivity of such species in the environment. Several of the many reaction processes as well as the solution-phase studies have begun in this lab, on the basis of this preliminary study.

TABLE 4: B3LYP/DZ+(2d,p) Calculated Dipole Moments (D) of Select Ethers and Amines

ROR' RNHR'	Me	Et	i-Pr	t-Bu
Me	1.379 1.062	1.266	1.393	1.303
Et	0.996	1.156 0.935	1.292	1.212
i-Pr	0.992	0.942	1.243 0.9053	1.2480
t-Bu	0.918	0.867	0.977	1.097 0.695

One may find it interesting to contemplate alternative sources to MTBE that might be considered as not only efficient gasoline oxygenates, but additionally sources that are less harmful to the environment. An additional class of compounds that might be investigated are the ketones. During the course of this work, an investigation by Prakesh[45] revealed a potential surrogate, isopropyl methyl ketone, that has shown promise as a potential replacement for MTBE. Ketones, in general, are used extensively as solvents. If one compares the structures of MTBE and isopropyl methyl ketone, the arrangements are such as to have nearly identical spatial overlay. However, the dipole moment of the latter structure, as one might expect, is much higher due to the carbonyl group (2.97 vs 1.30 for isopropyl methyl ketone vs MTBE, respectively). The polarization of the carbonyl functional group makes the boiling points of ketones in general higher than those of the analogous hydrocarbons. Because of their polarity, the smaller ketones are expected to be soluble in water; however, as the hydrophobic hydrocarbon moiety of the molecule increases in size, the water solubility decreases. Whether or not this is a viable replacement compound is left to further experimental and theoretical testing.

Acknowledgment. We acknowledge the National Institutes of Health (NIH PA1 RR08615-06) and the GAAN Foundation for support during this project. A generous donation from COMPAQ computers also allowed progress with some of this work, as well as an allocation of supercomputer time from the NSF SDSC/NRAC program.

References and Notes

(1) Chang, T. Y.; Hammerle, R. H.; Japar, S. M.; Salmeen, I. T. *Environ. Sci. Technol.* **1991**, *25*, 1190−1197.

(2) Japar, S. M.; Wallington, T. J.; Rudy, S. J.; Chang, T. Y. *Environ. Sci. Technol.* **1991**, *25*, 415−420.

(3) Clean Air Act, http://earth1.epa.gov/oar/oaq_caa.html.

(4) Schaffer, K. L.; Uchrin, C. G. *Bull. Environ. Contam. Toxicol.* **1997**, *59*, 744−749.

(5) U.S. Envronmental Protection Agency (EPA), http://www.epa.gov.

(6) Brown, S. L. *Regul. Tox*icol. Pharmacol. **1997**, *25*, 256−276.

(7) Mennear, J. H. *Risk. Anal.* **1997**, *17*, 673−681.

(8) Secretarys Scientific Advisory Board on Toxic Air Pollutants. *Env. Health Perspect.* **1995**, *103*, 420−422.

(9) Squillace, P. J. *Environ. Sci. Technol.* **1996**, *30*, 1721.

(10) Book, S. "Drinking Water Standards for MTBE"; State of California, Department of Health Services, 1998.

(11) Japar, S. M.; Wallington, T. J.; Richert, J. F. O.; Ball, J. C. *Int. J. Chem. Kinet.* **1990**, *22*, 1257−1269.

(12) Miyake, T.; Shibamoto, T. *Bull. Environ. Contam. Toxicol.* **1999**, *62*, 416−419.

(13) Konaka, S.; Takeuchi, H.; Siam, K.; Ewbank, J. D. *J. Mol. Struct.* **1990**, *222*, 503−508.

(14) Liedle, S.; Mack, H. G.; Oberhammer, H.; Imam, M. R.; Allinger, N. L. *J. Mol. Struct.* **1989**, *198*, 1−15.

(15) Suenram, R. D.; Lovas, F. J.; Pereyra, W.; Fraser, G. T. *J. Mol. Spectrosc.* **1997**, *181*, 67−77.

(16) Liang, S.; Palencia, L. S.; Yates, R. S.; Davis, M. K.; Bruno, J.-M.; Wolfe, R. *J.—Am. Water Works Assoc.* **1999**, *91*, 104−114.

(17) Aschmann, S. M.; Atkinson, R. *Products of the Gas-Phase Reactions of the OH Radical with n-Butyl Methyl Ether and 2-Isopropoxyethanol: Reactions of ROC(O) Radicals*; John Wiley & Sons: New York, 1999.

(18) Idriss, H.; Miller, A.; Seebauer, E. G. *Catal. Today* **1997**, *33*, 215−225.

(19) Schmidt, M. W.; Baldridge, K. K.; Boatz, J. A.; Jensen, J. H.; Koseki, S.; Gordon, M. S.; Nguyen, K. A.; Windus, T. L.; Albert, S. T. *QCPE Bull.* **1990**, *10*.

(20) Schmidt, M. W.; Baldridge, K. K.; Boatz, J. A.; Elbert, S. T.; Gordon, M. S.; Jensen, J. H.; Koseki, S.; Matsunaga, N.; Nguyen, K. A.; Su, S.; Windus, T. L.; Elbert, S. T. *J. Comput. Chem.* **1993**, *14*, 1347.

(21) Frisch, M. J.; Trucks, G. W.; Schlegel, H. B.; Gill, P. M. W.; Johnson, B. G.; Robb, M. A.; Cheeseman, J. R.; Keith, T. A.; Petersson, G. A.; Montgomery, J. A.; Raghavachari, K.; Al-Laham, M. A.; Zakrzewski, V. G.; Ortiz, J. V.; Foresman, J. B.; Cioslowski, J.; Stefanov, B. B.; Nanayakkara, A.; Challacombe, M.; Peng, C. Y.; Ayala, P. Y.; Chen, W.; Wong, M. W.; Andres, J. L.; Replogle, E. S.; Gomperts, R.; Martin, R. L.; Fox, D. J.; Binkley, J. S.; DeFrees, D. J.; Baker, J.; Stewart, J. P.; Head-Gordon, M.; Gonzalez, C.; Pople, J. A. *GAUSSIAN94-DFT*, Revision D.3; Gaussian, Inc.: Pittsburgh, PA, 1994.

(22) Roothaan, C. C. J. *Rev. Mod. Phys.* **1951**, *23*, 69−89.

(23) Head-Gordon, M.; Pople, J. A.; Frisch, M. J. *Chem. Phys. Lett.* **1988**, *153*, 503.

(24) Møller, C.; Plesset, M. S. *Phys. Rev.* **1934**, *46*, 618−622.

(25) Parr, R. G.; Yang, W. *Density Functional Theory of Atoms and Molecules*; Oxford University Press: New York, 1989.

(26) Becke, A. D. *Int. J. Quantum Chem.* **1983**, *23*, 1915−1922.

(27) Kohn, W.; Sham, L. J. *Phys. Rev.* **1965**, *140*, A1133−A1138.

(28) Becke, A. D. *Phys. Rev.* **1988**, *A38*, 3098.

(29) Lee, C.; Yang, W.; Parr, R. G. *Phys. Rev.* **1988**, *B37*, 785−789.

(30) Perdew, J. P.; Chevary, J. A.; Vosko, S. H.; Jackson, K. A.; Pederson, M. R.; Singh, D. J.; Fiolhais, C. *Phys. Rev. B* **1992**, *46*, 6671−6687.

(31) Adamo, C.; Barone, V. *J. Chem. Phys.* **1998**, *108*, 664.

(32) Binning, R. C., Jr.; Curtiss, L. A. *J. Comput. Chem.* **1990**, *11*, 1206−1216.

(33) Ditchfield, R.; Hehre, W. J.; Pople, J. A. *J. Chem. Phys.* **1971**, *54*, 724−728.

(34) Hariharan, P. C.; Pople, J. A. *Theor. Chim. Acta* **1973**, *28*, 213.

(35) Hehre, W. J.; Ditchfield, R.; Pople, J. A. *J. Chem. Phys.* **1972**, *56*, 2257.

(36) Dunning, T. H., Jr.; Hay, P. J. *Modern Theoretical Chemistry*; Plenum: New York, 1976.

(37) Kendall, R. A.; Dunning, T. H.; Harrison, R. J. *J. Chem. Phys.* **1992**, *96*, 6796.

(38) Woon, D. E.; Dunning, T. H. *J. Chem. Phys.* **1993**, *98*, 1358.

(39) Baldridge, K. K.; Greenberg, J. P. *J. Mol. Graphics* **1995**, *13*, 63.

(40) Bode, B. M.; Gordon, M. S. *J. Mol. Graph. Mod.* **1999**, *16*, 133−138.

(41) Jordan, K. D.; Paddon-Row: M. N. *J. Phys. Chem.* **1992**, *96*, 1188−1196.

(42) Suwa, A.; Ohta, H.; Konaka, S. *J. Mol. Struct.* **1988**, *172*, 275−290.

(43) Fjeldberg, T.; Lappert, M. F. *J. Mol. Struct.* **1986**, *140*, 209−217.

(44) Bartel, L. S.; Bürgi, H.-B. *J. Am. Chem. Soc.* **1972**, *94*, 5236.

(45) Prakash, G. K. G., Independent research investigation.